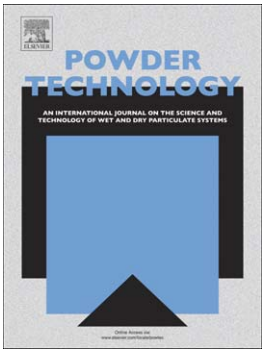

Optimization of gravity flow discharge chutes under the speed dependent resisting forces: maximizing exit velocity

Slaviša Šalinić, Aleksandar Obradović, Srdjan Rusov, Zoran Mitrović, Zoran Stokić

PII: S0032-5910(14)01033-X
DOI: doi: 10.1016/j.powtec.2014.12.051
Reference: PTEC 10712

To appear in: *Powder Technology*

Received date: 14 July 2014
Revised date: 22 December 2014
Accepted date: 28 December 2014

Please cite this article as: Slaviša Šalinić, Aleksandar Obradović, Srdjan Rusov, Zoran Mitrović, Zoran Stokić, Optimization of gravity flow discharge chutes under the speed dependent resisting forces: maximizing exit velocity, *Powder Technology* (2015), doi: 10.1016/j.powtec.2014.12.051

Optimization of gravity flow discharge chutes under the speed dependent resisting forces: maximizing exit velocity

Slaviša Šalinić[a,*], Aleksandar Obradović[b], Srdjan Rusov[c], Zoran Mitrović[b], Zoran Stokić[b]

[a] *University of Kragujevac, Faculty of Mechanical and Civil Engineering in Kraljevo, Dositejeva 19, 36000 Kraljevo, Serbia*
[b] *University of Belgrade, Faculty of Mechanical Engineering, Kraljice Marije 16, 11120 Belgrade 35, Serbia*
[c] *University of Belgrade, Faculty of Transport and Traffic Engineering, Vojvode Stepe 305, 11000 Belgrade, Serbia*

Abstract

Using the optimal control theory, the problem of finding profiles of gravity flow discharge chutes required to achieve maximum exit velocity of granular material under the speed dependent resisting forces is solved. A model of a particle moving down a curve which is treated as an unilateral constraint is used. The fast flow condition and the condition that the particle does not leave the curve are introduced as the additional inequality constraints. The influence of the initial particle speed and the power of the speed in the expression for the resisting force on the optimal chute profile is analysed.

Keywords: Discharge chutes, Maximum velocity, Optimal control, Resisting forces

*Tel.: +381 36 383269; fax: +381 36 383269
Email addresses: salinic.s@ptt.rs (Slaviša Šalinić), salinic.s@mfkv.kg.ac.rs (Slaviša Šalinić)

1. Introduction

This paper considers the problems of the optimization of gravity flow discharge chute profiles in bulk granular materials handling installations. Figure 1(a) displays a principle scheme of such an installation. From the bin (1), the granular material (2) moves by means of the feeder (3) into the loading chute (4). At the exit of the chute, the material is delivered to the conveyor (5) (note that some other storage device can be this component of the system). A granular material flows along a chute under the action of its own weight and that is why in the literature such chutes are called gravity flow discharge chutes. In chute profile optimization the most common optimization criteria are the minimization of the transit time of granular materials and the minimization of the losses of mechanical energy of granular materials due to the friction. The last criterion is often expressed as maximization of the exit velocity of the granular material. For the other optimization criteria for this type of installation see [1, 2].

Figure 1

In the reference [3] it was shown that in case when a material flows through a chute in the form of fast flow, the flow of material through the chute can be modelled as a particle M moving down a curve with tangentially directed resisting forces (see Fig. 1(b)). The curve is treated as an unilateral constraint because the open chutes are considered. This means that the particle must slide along the curve like a block on an inclined plane. The shape of this curve should be such that the particle M starting from the position $M_0(x_0, y_0)$ with the initial speed V_0 reaches the position $O(0, 0)$

either for the minimal time or the maximal speed (minimal losses of mechanical energy). In Fig. 1(b), y represents the vertical axis directed downwards, and x is the horizontal axis of a Cartesian coordinate system.

In the reference [4] considerations of the problem of maximum exit velocity of granular material under the speed dependent resisting forces do not take into account the fast flow condition and the condition that the particle does not leave the chute. Consequently, the results obtained in [4] refer to those values of the model's parameters that ensure the satisfaction of the previous conditions without their explicit incorporation in the equations of the problem. A similar problem, without connection with the problem of optimization of discharge chutes, was considered in [5]. The solution for the problem of maximum exit velocity under the Coulomb friction force as well as a review of literature relating to this problem is given in [6].

In this paper, using the optimal control theory [7, 8], the problem of maximization of exit velocity is solved by directly introducing the fast flow condition and the condition of non-leaving the chute bottom. To the best of the authors' knowledge, solving the considered problem by using these two conditions has not been reported elsewhere before. These conditions, considering the model of a particle used, are represented by equivalent conditions that the particle tangential acceleration is larger or equal to zero and that during motion the reaction of the chute does not change the direction. The resisting force that depends on the particle velocity is considered. The numerical procedure for solving the problem is based on the shooting method [9]. The determination of optimal chute profiles is illustrated via examples. The obtained chute profiles are compared with those existing in literature.

2. Optimal control formulation

The differential equation of motion of the particle M shown in Fig. 1(b) reads:

$$m\overrightarrow{a} = m\overrightarrow{g} + \overrightarrow{N} + \overrightarrow{F}_w. \tag{1}$$

where $\overrightarrow{a}$ is the acceleration of the particle, $\overrightarrow{g} = g\,\overrightarrow{j}$, g is the acceleration of gravity, $\overrightarrow{N}$ is the normal component of the constraint reaction force, and $\overrightarrow{F}_W$ is the resisting force.

Let us introduce the unit vectors $\overrightarrow{\tau}$ and $\overrightarrow{\sigma}$ in the following way [10] (see Fig. 1(b)):

$$\overrightarrow{\tau} = (\cos\varphi)\,\overrightarrow{i} + (\sin\varphi)\,\overrightarrow{j}, \tag{2}$$

$$\overrightarrow{\sigma} = \frac{d\overrightarrow{\tau}}{d\varphi} = (-\sin\varphi)\,\overrightarrow{i} + (\cos\varphi)\,\overrightarrow{j}, \tag{3}$$

where $\overrightarrow{i}$ and $\overrightarrow{j}$ are the unit vectors of axes x and y, respectively, and $\overrightarrow{\tau}$ and φ are the unit vector and the slope angle of the tangent to the particle path, respectively. It is obvious that $\overrightarrow{\tau} \cdot \overrightarrow{\sigma} = 0$. The reason to introduce vector $\overrightarrow{\sigma}$ is that the unit vector $\overrightarrow{\sigma}$, in contrast to the principal normal unit vector of the particle path, does not change the orientation with changing of the concavity of the curve and it is constantly directed to the same side with $\overrightarrow{g}$ (see Fig. 1(b)). Now, the acceleration $\overrightarrow{a}$ can be written as (see [10])

$$\overrightarrow{a} = \dot{V}\overrightarrow{\tau} + V\dot{\varphi}\overrightarrow{\sigma} \tag{4}$$

where an overdot denotes the derivative with respect to time t and V represents the projection of the particle velocity on the direction $\overrightarrow{\tau}$. Also, in regard to Fig.1(b), the following kinematics relations hold:

$$\dot{x} = V\cos\varphi, \qquad \dot{y} = V\sin\varphi. \tag{5}$$

In further considerations it is assumed that the force $\overrightarrow{F}_W$ has the following form:

$$\overrightarrow{F}_W = -mR(V)\overrightarrow{\tau} \tag{6}$$

where $R(V)$ is the resisting force per unit mass of the form

$$R(V) = \beta V^k. \tag{7}$$

In Eq.(7), β denotes the friction coefficient in dimension $\mathrm{m}^{1-k}/\mathrm{s}^{2-k}$ and $k \in R$. In regard to above, projecting (1) on the directions $\overrightarrow{\tau}$ and $\overrightarrow{\sigma}$ yields

$$\dot{V} = g\sin\varphi - \beta V^k\,, \tag{8}$$

$$mV\dot{\varphi} = mg\cos\varphi + N_\sigma, \tag{9}$$

where $N_\sigma = \overrightarrow{N}\cdot\overrightarrow{\sigma}$. In accordance to the lumped particle model used, the condition that the particle does not leave the curve can be expressed in the form

$$N_\sigma \leq 0, \tag{10}$$

and the condition that the flow of a granular material through the discharge chute is fast [3] can be expressed through the following equivalent condition imposed to the particle tangential acceleration:

$$\dot{V} \geq 0. \tag{11}$$

In order to formulate a optimal control task, let us introduce a new variable p and a control variable u as in [11]:

$$p \triangleq \tan\varphi\,, \quad u \triangleq \frac{dp}{dx}. \tag{12}$$

Now, in accordance to (5), (8), (12) and taking the quantities y, p, and V as states, the following state equations can be formed:

$$\frac{dy}{dx} = p, \tag{13}$$

$$\frac{dp}{dx} = u, \tag{14}$$

$$\frac{dV}{dx} \triangleq f_V(p,\, V) = \frac{gp - \beta V^k\sqrt{1+p^2}}{V}, \tag{15}$$

with the prescribed initial and terminal conditions

$$x = 0:\ y(0) = 0\,, \qquad V(0) = V_0\,; \qquad x = x_f:\ y(x_f) = y_f\,. \tag{16}$$

Now, from Eq. (9) it follows that

$$N_\sigma = \frac{muV^2}{(1+p^2)^{3/2}} - \frac{mg}{\sqrt{1+p^2}}. \tag{17}$$

Further, since

$$\dot{V} = \frac{dV}{dx}\frac{V}{\sqrt{1+p^2}} \tag{18}$$

and since it is in the nature of the problem posed that $V \geq 0$, then the condition (11) is equivalent to the condition

$$\frac{dV}{dx} \geq 0. \tag{19}$$

Now, based on (15) and (17), the inequalities (10) and (19) take the following form:

$$C_1(p,\, V,\, u) \triangleq \frac{uV^2}{(1+p^2)^{3/2}} - \frac{g}{\sqrt{1+p^2}} \leq 0, \tag{20}$$

$$S(p,\, V) \triangleq -gp + \beta V^k \sqrt{1+p^2} \leq 0. \tag{21}$$

Let $E = T + \Pi$ be the total mechanical energy of the particle, where $T = (1/2)mV^2$ and $\Pi = -mgy$ are the kinetic and potential energies of the particle, respectively. From the principle of work and energy for the particle one has

$$\frac{E(x_0) - E(x_f)}{m} = \int_0^{x_f} \beta V^k \sqrt{1+p^2}dx. \tag{22}$$

In regard to above, the posed problem consists in finding the control $u = u(x)$ and state variables $y = y(x)$, $p = p(x)$, and $V = V(x)$ that minimize the functional

$$J = \int_0^{x_f} \beta V^k \sqrt{1+p^2}dx \tag{23}$$

subject to the constraints (16), (20), (21).

3. Determination of the structure of the optimum chute profile

To determine the structure of the optimum chute profile, the same idea as in [4, 12] will be used. Namely, the problem is solved first provided that the constraints (20) and (21) are ignored temporarily. If an obtained solution satisfies these constraints then the same solution is valid for the case with the constraints (20) and (21) included. In this manner, initially, the chute profile is obtained representing a singular control of the first order [13]. Indeed, after the Hamiltonian [8]

$$H = \beta V^k \sqrt{1+p^2} + \lambda_y p + \lambda_p u + \lambda_V \frac{gp - \beta V^k \sqrt{1+p^2}}{V} \tag{24}$$

was formed, where λ_y, λ_p, and λ_V are the costate variables, the following costate equations are obtained:

$$\frac{d\lambda_y}{dx} \triangleq -\frac{\partial H}{\partial y} = 0 \ \rightarrow \lambda_y(x) = \text{Const}, \tag{25}$$

$$\frac{d\lambda_p}{dx} \triangleq -\frac{\partial H}{\partial p} = -\frac{\beta V^k p}{\sqrt{1+p^2}} - \lambda_y - \lambda_V \frac{g\sqrt{1+p^2} - p\beta V^k}{V\sqrt{1+p^2}}, \tag{26}$$

$$\frac{d\lambda_V}{dx} \triangleq -\frac{\partial H}{\partial V} = -\frac{k\sqrt{1+p^2}\beta V^k}{V} + \lambda_V \frac{gp + (k-1)\sqrt{1+p^2}\beta V^k}{V^2}, \tag{27}$$

with the transversality conditions [8]:

$$\lambda_p(0) = 0, \qquad \lambda_V(x_f) = 0, \qquad \lambda_p(x_f) = 0. \tag{28}$$

Since the control u appears linearly in the Hamiltonian H, the differentiation of the Hamiltonian H with respect to x is performed as long as the control u appears explicitly [8, 13]. After that, one obtains:

$$\frac{\partial H}{\partial u} = \lambda_p(x) \equiv 0\,, \tag{29}$$

$$\frac{d}{dx}\frac{\partial H}{\partial u} = -\frac{\beta V^k p}{\sqrt{1+p^2}} - \lambda_y - \lambda_V \frac{g\sqrt{1+p^2} - p\beta V^k}{V\sqrt{1+p^2}} \equiv 0. \tag{30}$$

The singular control u_{sing} is determined by differentiating (30) with respect to x:

$$u_{sing} = \frac{gk(1+p^2)}{V^2}. \tag{31}$$

The control (31) represents the first-order singular optimal control [13] for which Kelley's optimality condition [13] :

$$K \triangleq (-1)^n \frac{\partial}{\partial u}\left(\frac{d^2}{dx^2}\left[\frac{\partial H}{\partial u}\right]\right) \geq 0,\ n = 1 \tag{32}$$

has to be satisfied with $n \in N$ denoting the order of the singular optimal control. In a developed form, the condition (32) reads

$$K = \frac{\beta V^k (V - \lambda_V)}{V(1+p^2)^{3/2}} \geq 0. \tag{33}$$

Substituting (31) into (17) gives:

$$N_\sigma = \frac{mg(k-1)}{\sqrt{1+p^2}}. \tag{34}$$

On the other hand, for a subarc on the boundary $S = 0$, from Eq. (15) it follows that

$$V(x) = \text{Const.} \tag{35}$$

Also, based on (14) and (35), differentiating equality constraint $S(p, V) = 0$ with respect to x yields

$$u\left(-g + \frac{\beta V^k p}{\sqrt{1+p^2}}\right) = 0. \tag{36}$$

After incorporating $S = 0$ in the last relation, one obtains

$$S^{(1)} \triangleq u\left(-\frac{g}{1+p^2}\right) = 0 \tag{37}$$

from which it is obvious that

$$u = 0. \tag{38}$$

Substituting (38) into (14) gives

$$p(x) = \text{Const.} \tag{39}$$

which means that a subarc lying on the boundary $S = 0$ represents a straight line. Now, substituting (38) in (17) yields

$$N_\sigma = -\frac{mg}{\sqrt{1+p^2}}. \tag{40}$$

According to (40), along this constrained subarc, the constraint (20) is satisfied with strict inequality. Finally, for the constrained subarc $N_\sigma = 0$, the optimal control is obtained from the relation $C_1(p, V, u) = 0$ and reads:

$$u = \frac{g(1+p^2)}{V^2}. \tag{41}$$

If the singular extremal satisfies the inequalities (20) and (21), the problem is solved. If any of these inequalities is disturbed on some subintervals, it is convenient that on these subintervals the extremal lies either on the boundary $S = 0$ or $C_1 = 0$. Based on (34), for $k < 1$ along a singular arc the inequality (20) is satisfied, however, on the other side, it may happen that the inequality (21) is disturbed. Considering this fact, for $k < 1$ the optimum shape of the chute profile is a combination of a singular arc and the arc lying on the boundary $S = 0$. Based on the graph of the curve $S(p(x), V(x))$, where the functions $p(x)$ and $V(x)$ are determined for $u(x) = u_{sing}$, it can be estimated on which sections of a singular extremal the condition (21) is disturbed. Specially, for constant friction ($k = 0$) , it is obvious that (34) is reduced to (40) and, consequently, the optimal chute profile represents a straight line. On the other hand, if k takes the value $k = 1$, the singular extremal lies on the boundary $C_1 = 0$. In this case, it should be checked whether the condition (21) is disturbed on any section of a singular extremal. If it is not the case, then a singular extremal is a solution to the problem, and if it is, a procedure similar as in the case $k < 1$ is applied. Finally, if $k > 1$, then the condition (20) is disturbed on a singular extremal because, based on (34), $N_\sigma > 0$ holds. In regard to this, for $k > 1$, a singular extremal can not be a section of the optimal chute profile. In this case, the highest value of exit velocity would be achieved if the entire chute profile represents the constrained arc $N_\sigma = 0$. At the same time, it should be checked again for the possible disturbance of the condition (21) along this arc.

4. Numerical examples

4.1. The case $k = 0.5$

For $x_f = y_f = 1\,\mathrm{m}$, $k = 0.5$, $\beta = 0.25\,\mathrm{m}^{1/2}/\mathrm{s}^{3/2}$, solving Cauchy's problem of the state equations with the condition $y(x_f) = y_f$, $p(x_f) = p_f$, and $V(x_f) = V_f$ yields the following relations in numerical form:

$$y_0 = f_1(p_f,\, V_f), \qquad V_0 = f_2(p_f,\, V_f). \tag{42}$$

Using various values of the speed V_0 and numerical solving the nonlinear system (42) yields the values of the parameters V_f and p_f, which are shown in Table 1. The values of λ_y are calculated applying the relation (30) at the point $x = x_f$. Based on these data, in Figs. 2 and 3 the chute profiles and the the curves $S(p(x),\, V(x))$ are shown, respectively. Note that an arrow with designation V_0 indicates how chute profiles distribute in figures with growing value of V_0.

Table 1

Figure 2

Figure 3

Figure 4

The numerical confirmation of Kelley's condition (33) is presented in Fig. 4. From Fig. 3 it is obvious that as the value of velocity V_0 is reduced, the value $S(p_0,\, V_0)$ tends to zero, where $p_0 = p(0)$. For $V_0 = V_{0cr1} = 1.33689\,\mathrm{m/s}$, one has that $S(p_0,\, V_0) \approx 0$ as well as $V_f = 4.49156\,\mathrm{m/s}$, $p_f = 1.63987$, and

$\lambda_y = -0.452359\text{m/s}^2$. This means that with further reduction of initial speed, the constraint (21)is disturbed at the initial section of a singular arc. In regard to this, for $V_0 < V_{0cr1}$, the optimum chute profile begins with the constrained arc $u = 0$ and ends with the singular arc u_{sing}. To determine the transversality conditions as well as the corner conditions at a point $0 < x_1 < x_f$ where the constrained and singular subarcs join, the approach from [7] will be used. Accordingly, the state equality constraint $S(p, V) = 0$ is equivalent to the control equality constraint (37) and the point constraint

$$S(p_0, V_0) = 0. \tag{43}$$

Now, an augmented performance index is introduced as (see [7])

$$J^\star = \nu S(p_0, V_0) + \int_0^{x_1} \left[\hat{H} - \lambda_y \frac{dy}{dx} - \lambda_p \frac{dp}{dx} - \lambda_V \frac{dV}{dx}\right] dx + \int_{x_1}^{x_f} \left[H - \lambda_y \frac{dy}{dx} - \lambda_p \frac{dp}{dx} - \lambda_V \frac{dV}{dx}\right] dx \tag{44}$$

where ν is the constant Lagrange multiplier and $\hat{H}$ is the extended Hamiltonian [7] defined as

$$\hat{H} = \beta V^k \sqrt{1 + p^2} + \lambda_y p + \lambda_p u + \mu S^{(1)} \tag{45}$$

where $\mu(x)$ is the Lagrange multiplier. The stationarity condition $\triangle J^\star = 0$, where $\triangle(\cdot)$ denotes the noncontemporaneous variation [7, 14, 15] of the quantity $(\cdot)$, gives the following relations:

$$-\frac{\nu g}{1 + p_0^2} + \lambda_p(0) = 0, \tag{46}$$

$$H(x_1+0)=\hat{H}(x_1-0), \tag{47}$$

$$\lambda_V(x_f)=0, \quad \lambda_p(x_f)=0, \tag{48}$$

$$\lambda_p-\frac{\mu g}{1+p^2}=0,\ 0\le x\le x_1, \tag{49}$$

$$\lambda_y(x_1+0)=\lambda_y(x_1-0),\ \ \lambda_p(x_1+0)=\lambda_p(x_1-0),\ \ \lambda_V(x_1+0)=\lambda_V(x_1-0), \tag{50}$$

as well as costate equations on the interval $[0,\ x_1]$:

$$\frac{d\lambda_y}{dx}\triangleq-\frac{\partial\hat{H}}{\partial y}=0\ \rightarrow\lambda_y(x)=\text{Const}, \tag{51}$$

$$\frac{d\lambda_p}{dx}\triangleq-\frac{\partial\hat{H}}{\partial p}=-\frac{\beta V^k p}{\sqrt{1+p^2}}-\lambda_y, \tag{52}$$

$$\frac{d\lambda_V}{dx}\triangleq-\frac{\partial\hat{H}}{\partial V}=-\frac{k\sqrt{1+p^2}\beta V^k}{V} \tag{53}$$

where the relation (38) is included. For given V_0, the quantity p_0 can be calculated from (43) as

$$p(x)\equiv p_0=\frac{1}{\sqrt{\left(\frac{g}{\beta V_0^k}\right)^2-1}}. \tag{54}$$

See [7, 14] for details of calculating $\triangle J^\star$. Also, taking into account the fact that state variables are continuous at $x=x_1$, i.e.,

$$y(x_1{+}0) = y(x_1{-}0) = p_0 x_1,\ p(x_1{+}0) = p(x_1{-}0) = p_0,\ V(x_1{+}0) = V(x_1{-}0) = V_0, \tag{55}$$

as well as Eqs. (29), (38), and (50), it is easy to show that the relation (47) is identically satisfied.

Further, based on previous relations, solving the costate equations (52) and (53) yields:

$$\lambda_p(x) = \left(\frac{\beta V_0^k p_0}{\sqrt{1+p_0^2}} + \lambda_y \right) (x_1 - x)\,, \tag{56}$$

$$\lambda_V(x) = \frac{k\sqrt{1+p_0^2}\beta V_0^k}{V_0}(x_1 - x) - \left(\lambda_y + \frac{\beta V_0^k p_0}{\sqrt{1+p_0^2}} \right) \frac{V_0\,(1+p_0^2)}{g}. \tag{57}$$

Based on these relations, the relations for ν and $\mu(x)$ can be obtained from (46) and (49). The value x_1 is determined in accordance to the following numerical procedure. Namely, applying the Runge-Kutta method one solves in the interval $[x_f,\, x_1]$ Cauchy's problem of the state equations (13)-(15) with the singular control determined by (31) and the initial conditions $y(x_f) = y_f$, $p(x_f) = p_f$, $V(x_f) = V_f$. After that, the numerical dependencies $y(x_1) = f_3(x_1,\, V_f,\, p_f)$, $p(x_1) = f_4(x_1,\, V_f,\, p_f)$, and $V(x_1) = f_5(x_1,\, V_f,\, p_f)$ are established. Further, taking (55), the following nonlinear system of equations are obtained:

$$p_0 x_1 = f_3(x_1,\, V_f,\, p_f), \quad p_0 = f_4(x_1,\, V_f,\, p_f),$$

$$V_0 = f_5(x_1,\, V_f,\, p_f). \tag{58}$$

For $x_f = y_f = 1\,\mathrm{m}$, $k = 0.5$, $\beta = 0.25\,\mathrm{m}^{1/2}/\mathrm{s}^{3/2}$, and various values of the speed $V_0 < V_{0cr1}$, by numerically solving the equation system (58), the values of the parameters x_1, p_f, and V_f are obtained. These values are shown in Table 2, where $\varphi_0 = \arctan p_0$. The values of λ_y are calculated applying the relation (30) at the point $x = x_f$. Based on these data , the chute profiles and the numerical confirmation of Kelley's condition (33) are shown in Figs. 5 and 6, respectively. From Fig.5 and Table 2 it can be observed that the initial parts of optimum chute profiles have almost the form of a horizontal straight line.

Table 2

Figure 5

Figure 6

4.2. The case $k = 2$

In accordance with the conclusions presented in the last paragraph of Section 3, this case is initially solved assuming that the entire chute profile represents an arc along which $N_\sigma = 0$. Following the approach from [7], this can be treated as the problem of minimization of the functional (23) subject to the constraint (16) and the control equality constraint $C_1(p, V, u) = 0$. After introducing the following augmented performance index

$$J^\star = \int_0^{x_f} \left[\hat{H} - \lambda_y \frac{dy}{dx} - \lambda_p \frac{dp}{dx} - \lambda_V \frac{dV}{dx} \right] dx \tag{59}$$

where

$$\hat{H} = \beta V^k \sqrt{1+p^2} + \lambda_y p + \lambda_p u + \lambda_V f_V + \mu C_1, \tag{60}$$

the stationarity condition $\triangle J^\star = 0$ gives the costate equations:

$$\frac{d\lambda_y}{dx} \triangleq -\frac{\partial \hat{H}}{\partial y} = 0 \ \rightarrow \lambda_y(x) = \text{Const}, \tag{61}$$

$$\frac{d\lambda_p}{dx} \triangleq -\frac{\partial \hat{H}}{\partial p} = -\frac{\beta V^k p}{\sqrt{1+p^2}} - \lambda_y - \lambda_V \frac{g\sqrt{1+p^2} - p\beta V^k}{V\sqrt{1+p^2}} - \mu \frac{\partial C_1}{\partial p}, \tag{62}$$

$$\frac{d\lambda_V}{dx} \triangleq -\frac{\partial \hat{H}}{\partial V} = -\frac{k\sqrt{1+p^2}\beta V^k}{V} + \lambda_V \frac{gp + (k-1)\sqrt{1+p^2}\beta V^k}{V^2} - \mu \frac{\partial C_1}{\partial V}, \tag{63}$$

the transversality conditions (28) as well as

$$\lambda_p + \frac{\mu V^2}{(1+p^2)^{3/2}} = 0. \tag{64}$$

The state equations (13)-(15) and the costate equations (62) and (63) are integrated in the interval $[0,\, x_f]$ with the control u determined by (41). The following initial conditions $y(x_f) = y_f$, $p(x_f) = p_f$, $V(x_f) = V_f$, $\lambda_p(x_f) = \lambda_V(x_f) = 0$, and the following values of parameters $x_{x_f} = y_{x_f} = 1\,\text{m}$, $k = 2$, $\beta = 0.25\,\text{m}^{-1}$ are used. After that, a nonlinear system of equations are obtained:

$$y_0 = 0 = f_6(p_f,\, V_f,\, \lambda_y), \qquad V_0 = f_7(p_f,\, V_f,\, \lambda_y),$$

$$\lambda_p(0) = 0 = f_8(p_f,\, V_f,\, \lambda_y). \tag{65}$$

Using various values of the speed V_0, by numerically solving the system of equations (65), the values of the parameters V_f, p_f, and λ_y are obtained and presented in Table 3. Based on these data, in Figs. 7 and 8, the chute profiles and the curves $S(p(x), V(x))$ are shown, respectively.

Table 3

Figure 7

Figure 8

It is noticeable from Fig. 8 that the reduction of V_0 implies that the value $S(p_0, V_0)$ approaches to zero. For $V_0 = V_{0cr2} = 2.81846\,\mathrm{m/s}$ one has that $S(p_0, V_0) \approx 0$ as well as $p_f = 2.01042$, $V_f = 4.30058\,\mathrm{m/s}$, and $\lambda_y = -4.63171\mathrm{m/s}^2$. This means that for $V_0 < V_{0cr2}$, the optimum chute profile begins with the constrained arc $u = 0$ and ends with the constrained arc $N_\sigma = 0$. Similarly as in Sections 4.1, following approach from [7], the state equality constraint $S(p, V) = 0$ is replaced with the control equality constraint (37) and the point constraint (43). Also, the augmented performance index $J^\star$ reads

$$J^\star = \nu S(p_0, V_0) + \int_0^{x_1} \left[\hat{H}_1 - \lambda_y \frac{dy}{dx} - \lambda_p \frac{dp}{dx} - \lambda_V \frac{dV}{dx}\right] dx + \int_{x_1}^{x_f} \left[\hat{H} - \lambda_y \frac{dy}{dx} - \lambda_p \frac{dp}{dx} - \lambda_V \frac{dV}{dx}\right] dx \tag{66}$$

where the extended Hamiltonian $\hat{H}_1$ is given by:

$$\hat{H}_1 = \beta V^k \sqrt{1 + p^2} + \lambda_y p + \lambda_p u + \mu_1 S^{(1)}, \tag{67}$$

and where $\mu_1(x)$ is the Lagrange multipliers. Taking previous into account, from the stationarity condition $\triangle J^\star = 0$ it follows that

$$-\frac{\nu g}{1+p_0^2} + \lambda_p(0) = 0, \tag{68}$$

$$\hat{H}(x_1 + 0) = \hat{H}_1(x_1 - 0), \tag{69}$$

$$\lambda_p - \frac{\mu_1 g}{1+p^2} = 0,\ 0 \le x \le x_1, \quad \lambda_p + \frac{\mu V^2}{(1+p^2)^{3/2}} = 0,\ x_1 \le x \le x_f, \tag{70}$$

the costate equations (51)-(53) on the interval $[0,\ x_1]$, the costate equations (61)-(63) valid on the interval $[x_1,\ x_f]$, the last two transversality conditions from (28) as well as the relations (50), (54), and (55). Using (50) and (55), the condition (69) yields

$$\lambda_p(x_1) = 0. \tag{71}$$

Now, applying the similar procedure on the interval $[x_1,\ x_f]$ like for obtaining the system of equations (65), the following nonlinear system of equations are obtained:

$$p_0 x_1 = f_9(p_f,\ V_f,\ \lambda_y,\ x_1), \qquad V_0 = f_{10}(p_f,\ V_f,\ \lambda_y,\ x_1),$$

$$\frac{1}{\sqrt{\left(\frac{g}{\beta V_0^k}\right)^2 - 1}} = f_{11}(p_f,\ V_f,\ \lambda_y,\ x_1), \quad \lambda_p(x_1) = 0 = f_{12}(p_f,\ V_f,\ x_1,\ \lambda_y). \tag{72}$$

Using various values of the speed V_0, by numerically solving the system of equations (72), the values of the parameters V_f, p_f, x_1, and λ_y are obtained and presented in Table 4. The chute profiles corresponding to these values are shown in Fig. 9. At the end, using similar procedure as in Sect. 4.1, the expressions for $\lambda_p(x)$ and $\lambda_V(x)$ on the interval $[x_1, x_0]$ can be calculated. After that, the parameter ν is determined from (68). From Fig.9 and Table 4 it can be observed that decreasing of the value of V_0 is accompanied by the angle φ_0 approaches to zero value, i.e., the initial parts of optimum chute profiles take the form of almost a horizontal straight line.

Table 4

Figure 9

5. Conclusions

Using the optimal control theory, the optimum chute profiles that ensure the maximum exit velocity of granular material were obtained in this paper. It has been shown that the fast flow condition and the condition of non-leaving the chute bottom require that, in a general case, the chute profile be a two-segment curve. For values of initial speed larger than the corresponding critical values, the chute profile has the shape of a single-segment curve along which both conditions (20) and (21) are satisfied. It should be pointed out that in [4], the constraints (20) and (21) were not considered and that the considerations were restricted to the those values of parameters V_0, k, and β that enable the fulfilment of these conditions in a natural way. In regard to this, the results obtained in this paper represent generalization of

considerations and results reported in [4]. Note that the chosen control variable as well as the state variables enable to avoid the shooting of the costate λ_p and λ_V in the numerical procedure for solving the problem. This is of great importance because the costate variables, in principle, do not have a definite physical meaning and consequently it is not easy to guess beforehand the range of their values. Theoretical considerations presented in the paper also form a basis for considering the problem of minimization of the transit time of granular materials through discharge chutes. It is of importance to emphasize this in light of the fact that, to the best authors' knowledge, such kind of the problem of minimum time with the constraints (20) and (21) has not been previously considered in the literature.

Acknowledgements

This research was supported under Grant No. TR35006 by the Ministry of Education, Science and Technological Development of Serbia. This support is gratefully acknowledged.

References

[1] A.W. Roberts, Chute performance and design for rapid flow conditions, Chemical Engineering and Technology 26(2) (2003) 163-170

[2] C.M. Wensrich, Evolutionary optimisation in chute design, Powder Technology 138(2-3) (2003) 118-123.

[3] A.W. Roberts, An investigation of the gravity flow of noncohesive granular materials through discharge chutes, Transactions of ASME: Journal of Engineering for Industry 91(2) (1969) 373-381.

[4] R.D. Parbery, Chute profile for maximum exit velocity in gravity flow of granular material under velocity dependent friction, Journal of Powder and Bulk Solids Technology 3(3) (1979) 21-24.

[5] J. Vuković, On the determination of the constraints for the motion with the minimal loss of mechanical energy, in: Proceedings of the General Mechanics Symposium, 1994, Novi Sad, pp.31-38. (in Serbian)

[6] S. Šalinić, Analytical solution for the problem of maximum exit velocity under Coulomb friction in gravity flow discharge chutes, Archive of Applied Mechanics 80 (2010) 1149-1161.

[7] D.G. Hull, Optimal Control Theory for Applications, Springer-Verlag, New York, 2003.

[8] A.E. Bryson, Y.C. Ho, Applied Optimal Control, Hemisphere, New York, 1975.

[9] J. Stoer, J. Bulirsch, Introduction to Numerical Analysis, Springer-Verlag, Berlin, 1993.

[10] S. Šalinić, Contribution to the brachistochrone problem with Coulomb friction, Acta Mechanica 208(1-2) (2009) 97-115.

[11] O. Jeremić, S. Šalinić, A. Obradović, Z. Mitrović, On the brachistochrone of a variable mass particle in general force fields, Mathematical and Computer Modelling 54(11-12) (2011) 2900-2912.

[12] R.D. Parbery, Optimization of gravity flow discharge chutes for max-

imum exit velocity under Coulomb friction, Engineering Optimization 10(4) (1987) 297-307.

[13] H. Kelley, R.E. Kopp, G.H. Moyer, Singular Extremals, in: G.Leitmann (Ed.), Mathematics in Science and Engineering, Volume 31, Topics in Optimization, Academic Press, New York and London, 1967, pp.63-101.

[14] D.G. Hull, On the variational process in optimal control theory, Journal of Optimization Theory and Applications 67(3) (1990) 447-462.

[15] J.G. Papastavridis, Analytical Mechanics: A Comprehensive Treatise on the Dynamics of Constrained Systems; For Engineers, Physicists, and Mathematicians, Oxford University Press, 2002.

Table 1: Numerical values of the parameters of chute profiles for $k = 0.5$ and $V_0 > V_{0cr1}$

V_0 [m/s]	p_f	V_f [m/s]	λ_y [m/s^2]
3.0	1.27773	5.2133	-0.449514
2.0	1.42094	4.72298	-0.444311
1.5	1.55444	4.54063	-0.448018

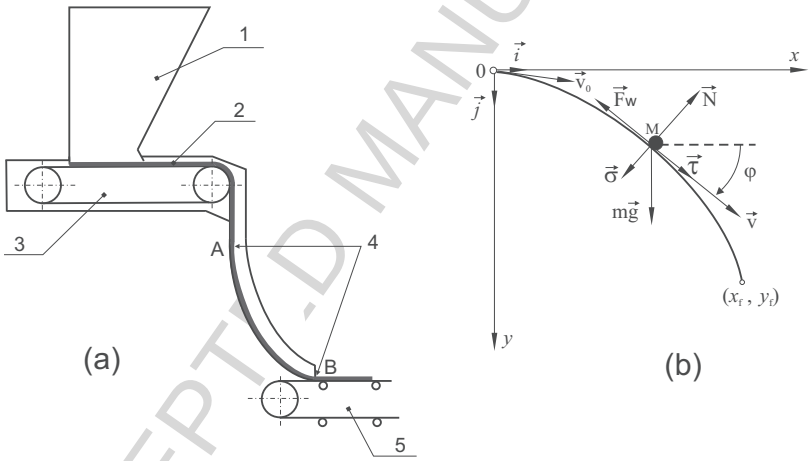

Figure 1: (a) Gravity flow discharge chute; (b) The physical model of the chute

Table 2: Numerical values of the parameters of chute profiles for $k = 0.5$ and $V_0 < V_{0cr1}$

V_0 [m/s]	p_f	φ_0 [°]	x_1 [m]	V_f [m/s]	λ_y [m/s^2]
1.1	1.8529	1.5	0.137616	4.43022	-0.463067
0.8	2.24345	1.3	0.314276	4.37042	-0.477363
0.5	2.93274	1.0	0.498437	4.33199	-0.492493

Table 3: Numerical values of the parameters of chute profiles for $k = 2$ and $V_0 > V_{0cr2}$

V_0 [m/s]	p_f	V_f [m/s]	λ_y [m/s^2]
3.5	1.74119	4.52688	-4.95527
3.2	1.84049	4.42143	-4.79612
3.0	1.92157	4.35608	-4.70367

Table 4: Numerical values of the parameters of chute profiles for $k = 2$ and $V_0 < V_{0cr2}$

V_0 [m/s]	p_f	φ_0 [°]	x_1 [m]	V_f [m/s]	λ_y [m/s^2]
2.0	2.67575	5.8	0.218298	4.09846	-4.2709
1.5	3.4837	3.3	0.389107	4.01538	-4.09945
1.0	5.13617	1.5	0.580008	3.96245	-3.96996

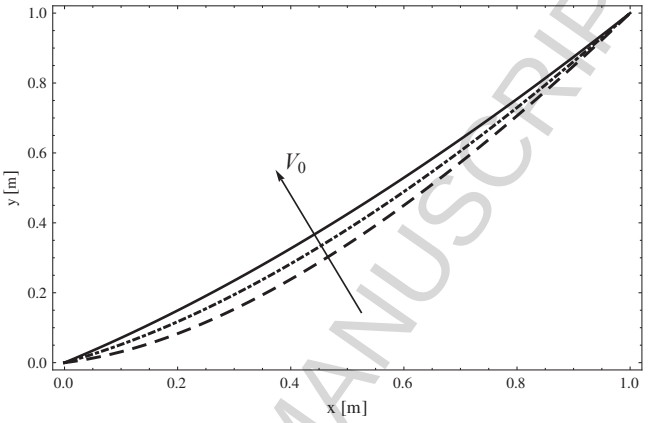

Figure 2: Optimum chute profiles corresponding to $k = 0.5$ and $V_0 > V_{0cr1}$

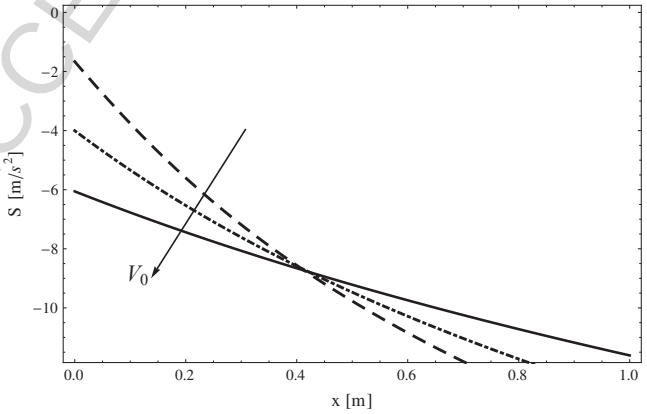

Figure 3: Graphs of the curve $S(p(x), V(x))$ corresponding to $k = 0.5$ and $V_0 > V_{0cr1}$

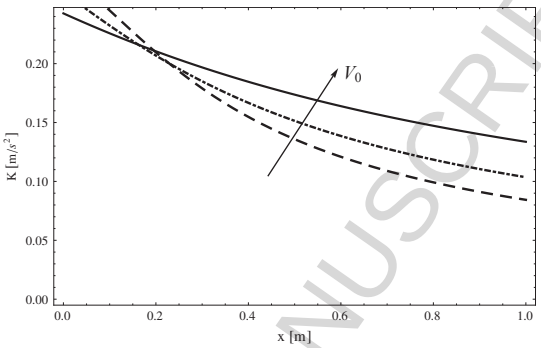

Figure 4: Numerical confirmation of Kelley's condition in the case of $k = 0.5$ and $V_0 > V_{0cr1}$

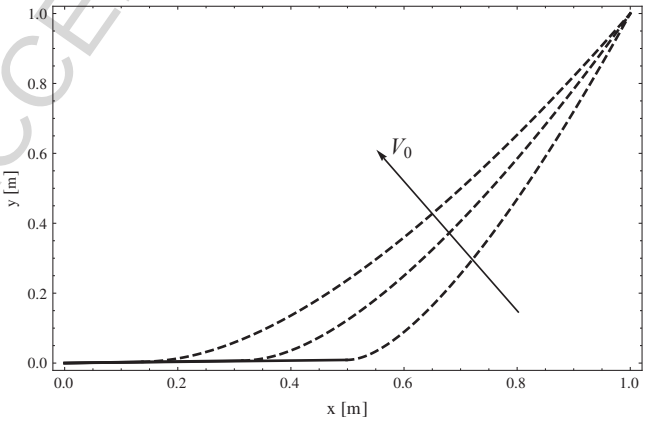

Figure 5: Optimum chute profiles corresponding to $k = 0.5$ and $V_0 < V_{0cr1}$

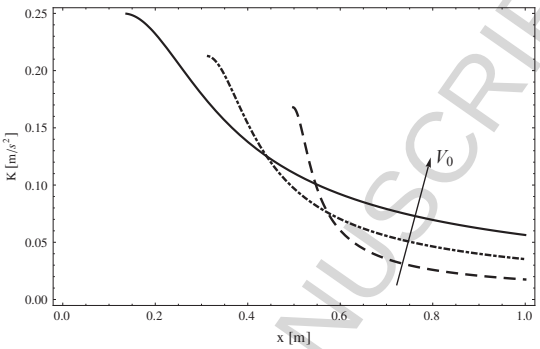

Figure 6: Numerical confirmation of Kelley's condition in the case of $k = 0.5$ and $V_0 < V_{0cr1}$

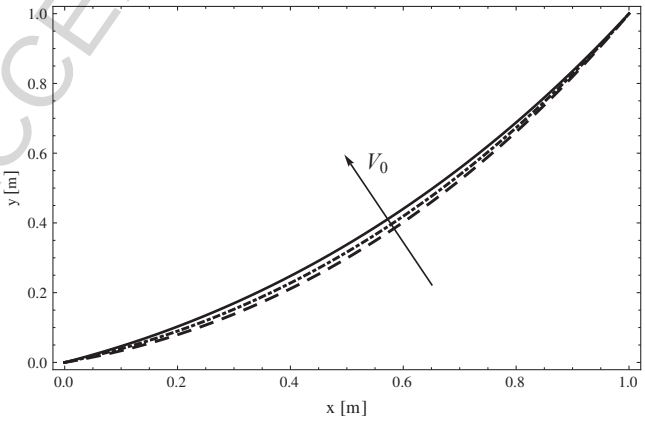

Figure 7: Optimum chute profiles corresponding to $k = 2$ and $V_0 > V_{0cr2}$

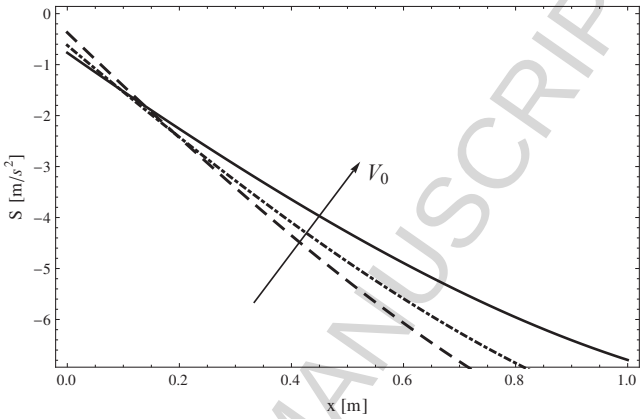

Figure 8: Graphs of the curve $S(p(x), V(x))$ corresponding to $k = 2$ and $V_0 > V_{0cr2}$

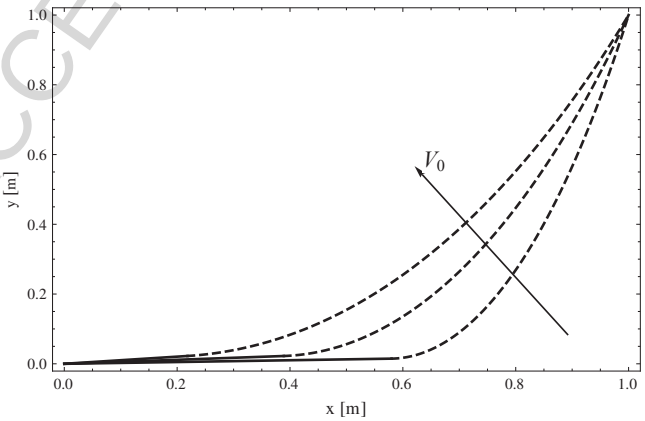

Figure 9: Optimum chute profiles corresponding to $k = 2$ and $V_0 < V_{0cr2}$

Highlights

The problem of chute profiles with maximum exit velocity is considered.

The optimization is based on the model of a particle moving down a curve.

The optimization problem is solved using the optimal control theory.

The optimal profiles represent, in general, two-segment curves.